

PAPER • OPEN ACCESS

Effects of low-grade gas composition on the energy/exergy performance of a polygeneration system (CH_2HP) based on biomass gasification and ICE

To cite this article: A Caricato *et al* 2022 *J. Phys.: Conf. Ser.* **2385** 012126

View the [article online](#) for updates and enhancements.

You may also like

- [A Search for Rapid Mid-infrared Variability in Gamma-Ray-emitting Narrow-line Seyfert 1 Galaxies](#)
Lisheng Mao and Tingfeng Yi
- [The Performance of Syngas-Fueled SOFCs Predicted by a Reduced Order Model \(ROM\): Temperature and Fuel Composition Effects](#)
Xinfang Jin, Anthony Ku, Atul Verma et al.
- [Experimental investigation of a non-catalytic cold plasma water-gas shift reaction](#)
Amit K Jaiswal, J Ananthanarasimhan, Anand M Shivapuji et al.

Effects of low-grade gas composition on the energy/exergy performance of a polygeneration system (CH_2HP) based on biomass gasification and ICE

A Caricato¹, A P Carlucci¹, A Ficarella¹, F Previtero¹, L Strafella¹, M Prestipino²,
A Galvagno² and S Brusca²

¹University of Salento, Dept. of Engineering for Innovation, via per Monteroni,
73100, Lecce, Italy

²University of Messina, Department of Engineering, C.da di Dio, 98166, Messina,
Italy

antonio.caricato1@unisalento.it, paolo.carlucci@unisalento.it,
antonio.ficarella@unisalento.it, francesco.previtero@studenti.unisalento.it,
luciano.strafella@unisalento.it, mauro.prestipino@unime.it,
antonio.galvagno@unime.it, sebastian.brusca@unime.it.

Abstract Bio-hydrogen from sustainable biomass (i.e. agro-industrial residues) gasification can play a relevant role in the hydrogen economy, providing constant hydrogen from renewable sources. Nowadays, most hydrogen production systems integrate one or more water-gas shift (WGS) units to maximize the hydrogen yield that, however, needs additional syngas treatments, investment and operational costs. Besides, different electricity inputs are needed along the process to power the compression of raw syngas, shifted syngas, and pure hydrogen to the desired pressure. This common process integration with WGS generates a kind of off-gas from the hydrogen separation unit whose composition may or may not be suitable for power production, depending on the operating conditions of the gasification unit. In this regard, this work proposes a different approach in which no WGS reactors are involved and the off-gas is used to generate heat and power to provide the energy input needed by the system. In particular, the authors tested the bio-syngas and the corresponding off-gas in a 4-cylinders, spark ignition natural gas internal combustion engine operated in cogeneration mode with the aim to analyse the effect of removing the hydrogen from the original bio-syngas on mechanical/electric and thermal power, on fuel efficiency and CO₂ specific emission.

1. Introduction

The growing energy demand required to meet the needs of the world population and the simultaneous reduction of conventional fossil energy sources pushes research towards the use of alternative fuels that are ecological, economical, efficient, and stable. A boost in this direction is also provided by the increasingly stringent regulations in terms of consumption and emissions. In fact, through the "Green Deal" agreement, the European Union is committed to reduce the consumption of fossil fuels and, in particular, by 2050, 60% of the global energy demand and 80% of the electricity needs must be guaranteed through renewable sources [1].



Among them, the gaseous mixtures deriving from the biomass gasification processes, the so-called synthesis gas or syngas, are of extreme importance. This fuel is basically composed of hydrogen, carbon monoxide, carbon dioxide, nitrogen and methane in highly variable compositions depending on the parameters involved in the gasification process [2]. For this reason, a distinction is generally made between:

- Producer gas, characterized by a high percentage of inert gases and a calorific value ranging between 4 and 7 $\frac{MJ}{kg}$. It is generally obtained through gasification processes in which the gasifying agent is air;
- Power gas, composed for the greater part of its volume by hydrogen and carbon monoxide. It is characterized by a calorific value between 10 and 28 MJ / kg and it results from gasification processes in which the gasifying agent is represented by pure oxygen or steam.

Through its use it is possible to achieve a cleaner combustion than the use of traditional liquid and solid fuels as, in general, no sulfur oxides (SO_x) are produced and, moreover, it releases a modest quantity of nitrogen oxides (NO_x), which are the main constituents of acid rain [3]. In addition, the environmental impact in terms of carbon dioxide is also greatly reduced, since syngas is a zero carbon fuel and, therefore, the carbon dioxide released during its combustion is equal to that absorbed by the biomass from which it derives [4]. Furthermore, a further feature that makes it extremely usable for energy production is the fact that its availability is not very variable with climatic conditions, as opposed to what happens for wind and solar energy, so its capacity appears to be almost constant in the medium term [5]. On the other hand, the Lower Heating Value (LHV) that characterizes the gaseous mixture penalizes the engine performance, with power derating generally between 20 and 35% [6].

1.1. Spark Ignition Engine fueled by syngas – A review

In the literature, numerous scientific studies have been conducted aimed at testing syngas as a fuel for spark ignition internal combustion engines in order to evaluate their outputs. For example, Indrawan et al. [7] analyzed the performance of a spark ignition (SI) engine fueled in its normal operating conditions with methane, feeding it with syngas (LHV = $6.45 \frac{MJ}{m^3}$). This study revealed a decrease in power of 28% but on the other hand a significant reduction in emissions of CO, NO_x , SO_x and HC. Gobbato et al. examined the performance of a heavy-duty SI engine fueled with extremely poor syngas, characterized by a LHV of $4.3 \frac{MJ}{kg}$ and a stoichiometric ratio of 1.15, from an energy point of view obtaining a derating of power of approximately 55 % compared to the case in which it is fed with methane [8]. Shah et al. [9] conducted a study with the aim to determine the performance and exhaust emission of a commercial 5.5 kW generator modified for operation with 100% syngas at different syngas flows and to compare the results with those obtained for gasoline operation at the same electrical power. The maximum electrical power output for syngas operation was 1.4kW and that for gasoline operation was 2.4 kW. However, the overall efficiency of the generator at maximum electrical power output for both fuels were found to be the same. The concentrations of CO and NO_x in the generator exhaust were lower for the syngas operation, respectively by 30–96% and 54–84% compared to the gasoline operation.

Other studies analyzed the performance of the engine by varying its fundamental characteristic parameters. For example, a study conducted by Nadaleti et al. [10] compared the performance and emission levels of a SI engine fueled with biogas, syngas and methane by varying ignition timing and air/fuel ratio. In particular, from this study it resulted that for both methane and biogas fuels, the increase in air excess ratio value from 1 to 1.25 led to lower CO and NO_x emissions as well as an increase in indicated efficiency. For both compositions of syngas, with an increase of λ (ratio between air and fuel with respect to the stoichiometric ratio of the fuel used), a reduction of NO_x emissions and an increase of indicated efficiency were obtained. Although the engine worked under lean mixture conditions, HC emissions were higher for all fuels analysed. Ran et al. [11] conducted an experimental study in which

a SI engine fueled with gasoline, ethanol, methane, and syngas was tested. From this study it emerged that using syngas it is possible to maintain stable combustion even with reaching extremely low fuel/air ratios, equal to 0.3, which leads to high thermal and combustion efficiency values with minimum CO emissions and zero virtual emissions of NO_x . The same conclusions were reached by a study conducted by Hagos et al. [12] where a SI engine was tested with natural gas and syngas at different air/fuel ratios. Homdoug et al. [13] conducted an experimental study aimed at evaluating the performance of the engine as the ignition timing varies in the range 20-50 before top dead center (BTDC) degrees in a speed range between 1100 and 1900 rpm. In this work, the optimum ignition timing of the small producer gas engine was between 20° to 25° BTDC at 1100 rpm, 25° to 30° BTDC at 1300 rpm, 32.5° to 37.5° BTDC at 1500 rpm and 40° BTDC of 1700 rpm.

1.2. Cogeneration plant fueled with syngas

Numerous studies have been developed to examine the performance of cogeneration (or “combined heat and power” - CHP) plants fueled with syngas based on SI engines. In particular, the main studies were conducted on actually existing plants (both experimental and commercial) rather than from the point of view of simulation through software [14]. Regarding the small and micro-cogeneration plants implemented in Italy, La Villetta et al. [15] conducted the experimental characterization of a micro-cogeneration system, called CMD ECO 20, based on the coupling of a downdraft gasifier with syngas cleaning devices, an internal combustion SI engine and an electric generator. This system is sized to provide maximum electrical and thermal power respectively equal to 20 kWe and 40 kWth. Patuzzi et al. [5] conducted a detailed screening of small-sized CHP plants located in South Tyrol, cataloging them according to their main characteristics such as, for example, the gasification technology used, the type of gasifier, the biomass used as raw material, the gasifying agent, the purification plant, and the type of engine used for the production of heat and energy. Pedrazzi et al. [16] presented a work in which they analyze the advantages that can be obtained from using a mixture of syngas and landfill gas as raw material for cogeneration plants. In particular, a plant located in the province of Reggio Emilia fed with gas landfill capable of producing approximately 2 MW of electrical power and 2.5 MW of thermal power was analyzed. The addition of syngas brings a series of improvements to the starting plant. First of all, from the point of view of the amount of energy produced, there is an increase in the electrical and thermal power of the plant of 1.8 MW and 2 MW respectively. Other research works analyzed the thermodynamic and environmental impacts of heat and power production from residual biomass gasification with a Life Cycle approach [17], showing the beneficial effects of integrating the gasification-CHP system with the fruit juice industry.

1.3. Case study

The growing interest in hydrogen in both the automotive and energy sectors has increased the interest in the research of different renewable primary resources to derive it from. To this regard, biomass gasification can play a relevant role as process exploiting renewable and programmable resources. Hydrogen can be separated from the syngas stream generated into gasifiers through different processes. However, the most used one in the industrial field and which allows to obtain pure hydrogen up to 99.9%, is the so-called "Pressure Swing Adsorption" (PSA) through which hydrogen is extracted through adsorption processes [18]. In particular, it takes place inside special pressurized tanks by means of particular materials capable of selectively adsorbing the gases to be removed, which are accumulated on the bottom of the tank and are cyclically discharged into the environment [19]. Therefore, from this process, in addition to hydrogen, a further gaseous waste mixture is produced, called "Adsorbate gas", "PSA tail-gas" or "PSA off-gas" characterized by a certain energy content, being composed, in addition to inert materials (carbon dioxide and nitrogen), of carbon monoxide, methane and residual hydrogen.

The proposed system (Figure 1) consists of a gasification unit fed by residual biomass where air and steam are used as gasification mediums, a hydrogen separation unit, and an internal combustion engine for combined heat and power, which is fed by the PSA off-gas. The scope of the proposed process configuration is to obtain an off-gas that is able to provide the heat needed to dry wet residual biomass

(such as residues from the food&drink industry), and the electricity needed to power the compressors, and all the auxiliary units of the biomass conversion process, minimizing or avoiding the use of external energy input. Heat demand for citrus peel drying was previously calculated by Galvagno et al. [20], which is 5.1 MJ per kilogram of biomass on a dry basis to reduce the water content to 15%. The power demand consists of two main contributions, the electricity for syngas and hydrogen compression and the auxiliaries of the gasification unit. The latter is defined in the literature as 0.67-0.69 MJ per kilogram of biomass on a dry basis [20]. The power demand for compression has been defined by process simulation using the AVEVA PRO/II simulation software.

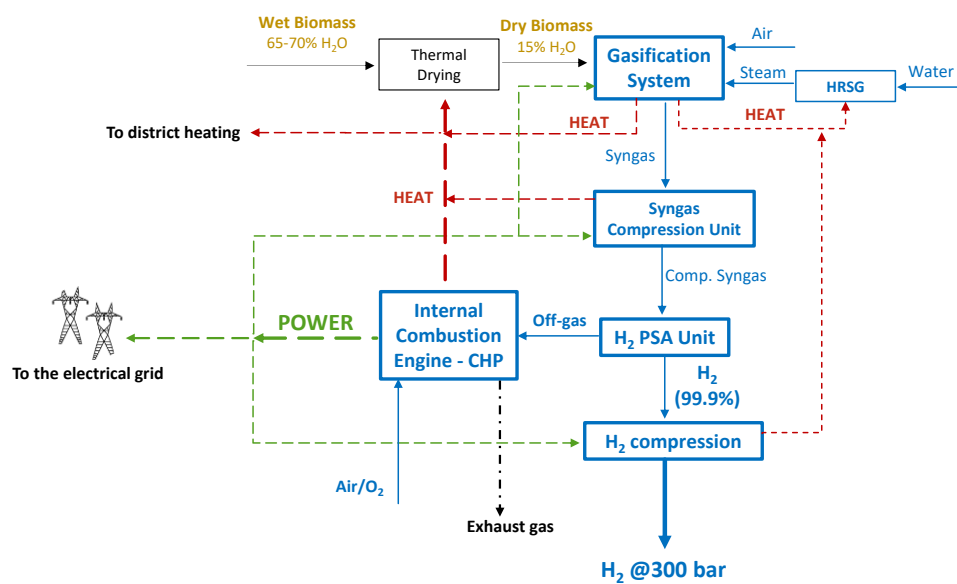


Figure 1. Layout of the proposed bio-hydrogen production system.

From the scientific literature concerning the use of the PSA off-gas, it emerged that there are few studies in which it is used for energy production in Internal Combustion Engine (ICE). For example, in the two Austrian plants of Güssing and Oberwart [21], the possibility of using this gaseous waste in a SI ICE is presented, without however examining the ways in which this can be done. However, given the continuous search for clean and renewable alternative fuels, the use of off-gas represents an opportunity, despite it is characterized by an extremely low calorific value and a stoichiometric mixture ratio close to 1. For this reason, an experimental study was conducted to evaluate the performance of a 4T Spark ignition engine in cogeneration mode fueled with this gaseous mixture, whose characteristics are presented in detail in the following paragraph.

The composition of syngas and off-gas used to feed engine (reported in **Table 2**) derive from process simulations of citrus peel gasification carried out using the AVEVA PRO/II Simulation software. The model used in this work is thermodynamic, based on the minimization of the Gibbs free energy of the chemical components involved into the conversion process. The model of the gasification unit is validated by experimental data obtained in previous research works on citrus peel gasification [20][22]. The gasification unit modeled in this work is operated at 850°C, Equivalence Ratio (ER) 0.3, and Steam to Biomass ratio (S/B, the mass flow rate ratio of steam and biomass on a dry basis) 0.125. The PSA is modeled considering 70% of hydrogen recovery efficiency, while the inlet pressure of the syngas stream is 7 bar [23]. In addition to the cogenerate heat in the CHP unit, heat recovery is performed by cooling the syngas that exits the reactor (after providing heat to the gasification agents), and by cooling the syngas and hydrogen in the corresponding compression units. The whole hydrogen production process described in Figure 1 (excluding the CHP unit) is simulated using the same simulation software as well. A more detailed description of the simulation model is reported by Prestipino et al. [24].

2. Experimental set-up

2.1. Internal combustion engine characterization

The tested engine is a 4-stroke 4-cylinder SI automotive-derivation engine whose main characteristics are shown in **Table 1**. The engine is designed to operate with natural gas.

Table 1. Engine characteristics.

Bore [mm]	72
Stroke [mm]	84
Displacement [cm ³]	1368
Power [kW]/[CV]	51/70
Torque [Nm]	104
Compression ratio	11.1:1

The PSA off gas was produced in the laboratory using an appropriate gas mixer (described in previous works [25][26]) and the choice of its composition was based on the study of the scientific literature in this field. **Figure 2** shows the layout of the mixer circuit, composed by the gas cylinders (containing hydrogen, methane, carbon monoxide, nitrogen and carbon dioxide), the mixer itself and the pressurized tank in which the mixture is stored. From here the off-gas is sent directly to the engine via a suitable supply line.

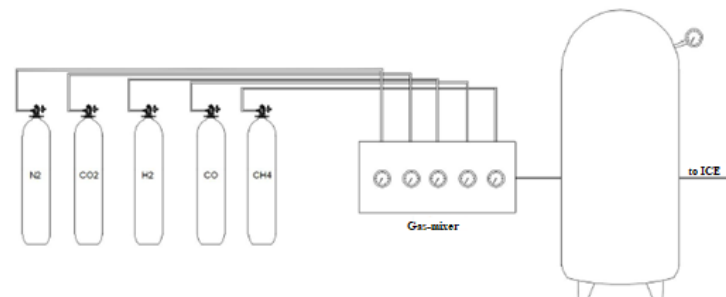


Figure 2. Gas mixer circuit.

The off-gas properties have been calculated using the following formulas which, given the volume or mass percentages of the gases that make up the mixture, return its density (ρ), specific heat capacity (c_p), Lower Heating Value and stoichiometric ratio, as in Equation (1), (2) and (3).

$$\rho_{off-gas} = \sum_i \%v_i \cdot \rho_i \left[\frac{kg}{m^3} \right] \quad (1)$$

$$c_{p,off-gas} = \sum_i \%m_i \cdot c_{p,i} \left[\frac{J}{kgK} \right] \quad (2)$$

$$LHV_{off-gas} = \sum_i \frac{m_i}{m} LHV_i \left[\frac{MJ}{kg} \right] \quad (3)$$

The fuel flow rate was calculated indirectly. In particular, from the indication of the stoichiometric condition reached provided by the lambda sensor and from the measurement of the intake air flow rate, knowing the stoichiometric ratio of the mixture, it is possible to calculate the fuel flow rate.

The engine was equipped with adequate instrumentation in order to detect the data useful for the analysis. In particular, a dynamic eddy current engine brake was used to measure the engine torque for each rpm set and then the output power. CO₂ emissions were measured through an AVL AMA i60 emission analyzer. Output data, provided in ppm, were converted in g/kWh based on SAE J1003 Standard.

Fuel conversion efficiency was estimated using the following formula:

$$\eta_f = 100 \cdot 3.6 \cdot \frac{P_u}{\dot{m}_f \cdot H_i} \quad (4)$$

Where:

- P_u = engine output power in [kW];
- \dot{m}_f = fuel mass flow rate in $\left[\frac{kg}{h}\right]$;
- H_i = Lower Heating Value in $\left[\frac{MJ}{kg}\right]$.

The engine was equipped with three thermocouples, which measure the temperature of the intake air, gaseous fuel and exhaust gases downstream the three-way catalyst respectively, and with an air mass flow sensor, which measures the air flow rate inside the engine.

Furthermore, the pressure inside the cylinder is measured by means of a piezoelectric pressure sensor embedded into the spark plug. For the correct acquisition and reading of the piezoelectric signal supplied by the spark plug, it was necessary to resort to an adequate instrumentation. In particular, the fulcrum of this set up is represented by AVL Indimicro, a signal amplifier that also acts as a data acquisition system.

Finally, since the engine under analysis works in cogeneration mode, the amount of thermal power that can be recovered from the engine cooling fluid and from the exhaust gases is extremely important. The cooling circuit is composed of two circuits in which water circulates and the heat exchange takes place in a counter-current heat exchanger. To measure the temperatures of the refrigerant fluid, two thermocouples are installed respectively at the inlet and outlet of the heat exchanger. To measure the heat output, it is also necessary to measure the flow rate flowing through the heat exchanger in addition to the temperature difference of the fluid. In this case, the fluid flow rate is measured through two CALEFFI meters with different capacities: DN 20 and DN 32, whose operating principle is based on the Venturi effect. From the knowledge of the pressure drop, displayed through two differential pressure gauges, it is possible to derive the flow rate through the characteristic curve of the instruments [27].

The recoverable thermal power of the exhaust gases is evaluated starting from the chemical composition of the latter. For its calculation, it was evaluated the product between the specific enthalpy of the exhaust gases and the flow rate of the same, obtained as the sum of the intake air flow and the fuel flow. The specific enthalpy of the mixture is the sum of the specific enthalpy of each component present. It is obtained as follows (Equation (5)):

$$\Delta h_i = y_i \int_{T_{min}}^{T_u} c_p(T) dT \quad \left[\frac{kJ}{kg}\right] \quad (5)$$

in which:

- y_i is the mass fraction of the i-th component of the mixture;
- $c_p(T) = a + bT + cT^2$. It is the specific heat at constant pressure in the hypothesis of perfect gas. The coefficients a, b, c are constants tabulated as a function of the i-th component;

- T_u and T_{min} are respectively the engine-out temperature of the exhaust gases and 383 K which is considered as the minimum temperature the exhaust gases can be brought.

2.2. Performance of the polygeneration system

The performance of the whole polygeneration system is assessed in terms of energy yields (Y_{Ei}) [MJ/kg] and hydrogen mass yield per unit of biomass Y_{mH2} [kg/kg], as reported in the following equations, where E_i describes the i -th energy stream (heat, electricity, and hydrogen) and m_{biom} is the mass of biomass on a dry basis. In this work, the energy yields are intended as the yield of net energy streams after covering the internal demands.

$$Y_{Ei} = \frac{E_i}{m_{biom}} \quad (6)$$

The cogenerated heat carrier is hot water at 393 K and 2.5 bar, which is obtained from heat recovered in the gasification and hydrogen separation units, as well as in the CHP unit where heat is recovered by cooling the engine and exhaust gas to 423 K.

The thermodynamic performance is assessed by the energy and exergy efficiencies of the whole system. The energy/exergy input considered in this work are the biomass (E_{biom}), the electricity (E_{el}) to power the gasification and compression units, and the natural Gas (E_{NG}) used to increase the lower heating value of the offgas up to the value obtained for the corresponding syngas (about 5.07 MJ/kg) and to cover the heat demand of the polygeneration system (drying and heating the gasification agents).

The electricity input is intended as electricity from the grid that is needed in the case the cogenerated one is not sufficient.

The output of the system are the net cogenerated electricity (E_{elCHP}), the net heat (E_{th}), and hydrogen (E_{H2} , LHV base). The net electricity and heat are the residual energy streams that can be exported after covering the internal demands.

$$\eta_{system} = \frac{E_{elCHP} + E_{th} + E_{H2}}{E_{biom} + E_{el} + E_{NG}} \quad (7)$$

$$\eta_{ex_system} = \frac{E_{ex_elCHP} + E_{ex_th} + E_{ex_H2}}{E_{ex_biom} + E_{ex_el} + E_{ex_NG}} \quad (8)$$

The exergy of natural gas and biomass are calculated considering their chemical exergies only, while the exergy of hydrogen compressed at 300 bar is calculated by summing the chemical and the physical exergies. The following equation is used to calculate chemical exergy of biomass:

$$E_{ex_biom} = 1.047 HHV_{biom} \quad (9)$$

Where HHV_{biom} refers to the higher heating value of biomass on a dry basis.

In the case of perfect gas, the physical exergy is calculated according to following equation:

$$E_{ex_ph} = mc_{pm} \left(T - T_0 - T_0 \ln \frac{T}{T_0} \right) + RT_0 \ln \frac{P}{P_0} \quad (10)$$

Where the subscript 0 refers to the reference state.

The exergy associated with heat recovery is calculated according to Equation 11, where Q is the heat exchanged, while T_0 and T_j are the temperature of the reference state and the temperature of the hot stream input, respectively.

$$E_{exQ} = \left(1 - \frac{T_0}{T_j} \right) Q \quad (11)$$

Along with the efficiencies and the energy yields, the direct Greenhouse Gases (GHG) impacts [$\text{CO}_2\text{-eq}$] of the proposed bio-hydrogen production are assessed. The biogenic CO_2 emissions are considered as carbon-neutral, so they do not contribute to the GHG impacts, as reported in Equation 12

$$GHG_{H_2} = \frac{E_{el}f_{el} + E_{NG}f_{NG} - (E_{elCHP}f_{el} + \frac{E_{th}}{0.9}f_{NG})}{m_{H_2}} \quad (12)$$

where f_{el} and f_{NG} stands for the emission factor of electricity from the national grid in Italy and the emission factor for natural gas combustion, respectively. In accordance with Eq. 8, the cogenerated electricity and heat are considered as substitutes of the electricity from the national grid and the one of natural gas used in a gas boiler with 90% thermal efficiency. The emission factors for electricity and natural gas are obtained from the Italian Superior Institute for the Environmental Research and Protection (ISPRA) [28].

3. Results

3.1. Internal Combustion Engine

The engine has been tested using different fuels, whose composition is reported in the following table:

Table 2. Gaseous fuels tested in the Internal Combustion Engine.

Fuel	H ₂ [%]	CO [%]	CO ₂ [%]	N ₂ [%]	CH ₄ [%]	Stech. ratio	LHV [MJ/kg]
Syngas	20	19	12	45	4	1.6	5.50
Off-gas_2	6	21	13	52	8	1.5	4.98
Off-gas	10	11	21	47	11	1.6	5.20
Methane	/	/	/	/	100	17.4	50

The off-gas_2 composition has been obtained eliminating most of the H₂ from the syngas composition. It stems from a steam to biomass ratio (S/B) equal to 0.12. On the other hand, a further – higher – S/B ratio was simulated with the aim of increasing the H₂ content. The corresponding off-gas has been labeled as “off-gas” in **Table 2**. Finally, the “all methane” case has been also reported as reference. As previously said, the tested engine, employed for land propulsion, was originally equipped with natural gas port fuel injection (PFI) system. Later on, the fuel supply system was replaced by a carburetor and the engine was fully characterized using methane. The results of this characterization, in terms of output power, thermal power released at the exhaust and thermal power exchanged with the cooling fluid, are reported in [27]. Then, the engine was fed – keeping the carburetor unchanged – using the syngas. In these conditions, it was possible to stably operate the engine only up to 10% of throttle. At 15% the engine could be operated stably but it was impossible to reach the stoichiometric ratio. As visible from **Table 2**, in fact, switching from methane to syngas determines a totally different mixing ratios between air and fuel. Most probably the stoichiometric ratio was not reached because the carburetor was not designed to operate with this different mixing ratio. As expected, the same problem arose feeding the engine with off-gas_2 and off-gas. Therefore, in this publication, only a comparison of experimental results obtained at 10% throttle will be shown.

In **Figure 3(a)** the in-cylinder pressure curves are compared for the four fuels. As visible, the two off-gases determine values globally lower than syngas and methane cases. It can be noticed that the combustion phase starts well before the Top Dead Center, so determining a high compression work. This could be probably limited delaying the spark advance, but during this experimental activity this aspect was not analyzed.

The output power is comparable between syngas and off-gas cases (see **Figure 3(b)**); in detail, a slight reduction is observed when off-gas_2 is employed. This, obviously, is due to the similar chemical properties that characterize the three mixtures. Furthermore, from the comparison of the power supplied by the engine in the cases in which it is fed with syngas, off-gas and off-gas_2 respect to methane, it emerges that the derating is approximately equal to 48%, 50.5% and 61.2% respectively. This reduction in power, to be asserted to the lower calorific value that characterizes gaseous mixtures, is however mitigated by the lower stoichiometric ratio and this means that the power in the three cases is of the same order of magnitude. In **Figure 3(c)** the fuel conversion efficiency is reported. It can be observed that the highest efficiency is achieved if methane is used, with values that settle at around 22.8%. The efficiencies are significantly reduced if off-gas and off-gas_2 are used, with reached values of 14.5% and 12% respectively. Finally, if syngas is used, the overall efficiency is around 17.6%. The gradual reduction in efficiency detected by switching from syngas to offgas_2 derives from the lower power delivered by the engine, compared to a similar calorific value and a similar fuel flow rate. Finally, in **Figure 3(d)** the CO_2 emission levels are plotted. It can be observed that in cases where the engine is powered by syngas and the two off-gas mixtures, the carbon dioxide emissions are higher. This derives from the fact that a considerable part of the CO_2 in the exhaust is that present in the initial composition of the gas. In fact, off-gas 2, which is composed of CO_2 for 52% by volume, has the highest emission values. In particular, using the syngas, off-gas and off-gas_2 mixture, the emissions achieved compared to methane are 1.5, 2.5 and 3.2 times higher. On the other hand, this aspect is not penalizing as syngas and off-gas produce zero net emissions of carbon dioxide as the CO_2 released during the combustion phase is the same as that absorbed by the biomass from which it derives.

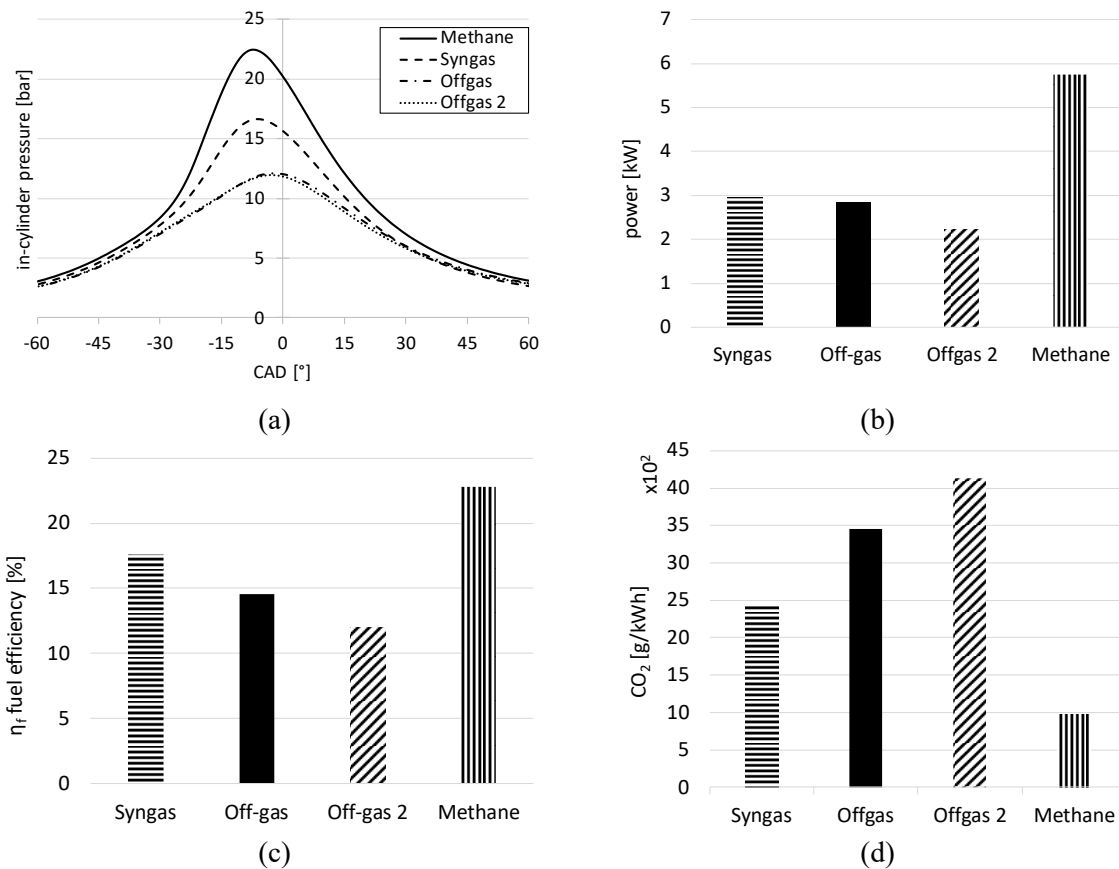


Figure 3. Comparison of ICE performance (1550rpm - 10% throttle) working with different fuels: a) in-cylinder pressure; b) output power; c) fuel conversion efficiency; d) CO_2 specific emissions.

3.2. Polygeneration system

From the experimental tests, it emerges the difficulty in testing the engine under full load condition. On other hand, the engine tested is a stationary engine so it never works at partial load. For this reason, a value for electrical efficiency of the cogeneration unit and a heat-to-power ratio at full load were respectively imposed equal to 30% and 1,14 as the ones resulting from a previous work conducted on the same engine operating in the same conditions - in terms of engine speed and throttle % - fed with methane [27]. These data are included in the model of the polygeneration system to assess the thermodynamic and environmental performance. The results of the system analysis are reported in **Table 3** at two different operating conditions of the gasification unit. In particular, the temperature was fixed at 1123 K, while two steam to biomass ratio (S/B) are investigated. The results shows that net electricity and heat can be cogenerated. At S/B=1.25, the cogenerated heat is much lower than the other condition due to the increased heat demand to generate the additional steam for the gasification process. As expected, the hydrogen yield (Y_{H2}) increases with the S/B, reaching 4.85 MJ/kg_{biom}, corresponding to 0.041 kg_{H2}/ kg_{biom}. The energy efficiencies are slightly reduced when moving from S/B=0.12 to S/B=1.25. The reported efficiency reduction is related to the lower net heat that is available. In the case of exergy efficiency, the higher the S/B the higher the efficiency. This behaviour is due to the increased hydrogen yield, which has high exergy/energy ratio. The lower net heat production at high S/B does not have a sensitive effect on the exergy efficiency due to the low exergy/energy ratio of hot water at 393 K.

The GHG emissions are negative at S/B=0.12, meaning that more non-biogenic GHG emissions are avoided than emitted by using NG to increase the LHV of the offgas entering the internal combustion engine. The avoided GHG emission are due to the substitution operated by the cogenerated net heat and power. Because of the low efficiency of the ICE, at S/B=1.25 the GHG emissions are positive, meaning that the cogenerated streams do not avoid enough GHG emissions than the ones caused by the addition of NG in the offgas stream.

Table 3. Energy Yields, Energy/Exergy efficiencies and GHG impacts of the proposed polygeneration systems.

S/B	Y_{Eel} [MJ/kg _{biom}]	Y_{Eth} [MJ/kg _{biom}]	Y_{H2} [MJ/kg _{biom}]	η_{system}	η_{ex_system}	GHG_{H2} [kgCO ₂ - eq/kg _{H2}]
0.12	2.060	1.197	3.000	0.307	0.240	-1.769
1.25	2.131	0.116	4.850	0.300	0.273	+5.152

Conclusions

This work presented an alternative system layout of a polygeneration system for bio-hydrogen production based on biomass gasification. In particular, the paper stressed the role of the energy valorisation of the low-grade gas in an internal combustion engine. The low-grade gases are the offgas obtained after hydrogen separation from the syngas stream.

The results of the system's performance showed that high steam-to-biomass ratio (S/B) reduces the net available heat due to the increased internal heat consumption and at the same time increases the Greenhouse gases (GHG) impacts of biohydrogen production, leading to high non-biogenic carbon emissions per unit of hydrogen mass. Increasing the S/B from 0.12 to 1.25, it causes a shift from negative to positive carbon emissions due the synergistic effects of increasing the natural gas (NG) consumption in the ICE and the reduction of net heat production, which is used as substitute for NG in NG-fed boilers. In terms of GHG emissions, the best performing conditions are obtained at S/B=0.12 (-1.769 kgCO₂-eq/kg_{H2}), due to the lower request of NG in the internal combustion engine, compared to the case of higher S/B. However, the highest exergy efficiency is reached at S/B = 1.25 because more syngas is converted to hydrogen, which is not subjected to additional conversion in the ICE.

This work showed the limitations of the existing ICEs when low-grade fuels are used. In particular, the parameter which most influences the behavior of the engine is the reduced stoichiometric ratio which means that a large quantity of gas must be sent inside the cylinders. Against this, the stoichiometric conditions were reached at 10% of the throttle opening, with reduced performance compared to the case in which methane is used.

With regard to carbon dioxide emissions, higher values were detected due to the presence of this element within the fuels themselves. Despite this, the environmental impact is zero since the amount of CO_2 emitted during combustion is the same as that captured by the starting biomass.

The performance of the proposed polygeneration system can be improved by applying proper modifications to the intake device, aiming at supplying a higher amount of fuel to the engine to reach the stoichiometric conditions at high loads. Furthermore, in this work the authors assumed the use of NG for increasing the quality of the offgas, but additional environmental improvements can be achieved if biomethane or biogas are used instead.

References

- [1] Li X, Pang Y, Tu H, Torrigino F, Biollaz S M A, Li Z, Huang Y, Yin X, Grimm F and Karl J 2021 *Energy Convers. Manag.* **250** 1–18
- [2] Fiore M, Magi V and Viggiano A 2020 *Appl. Energy* **276** 1–26
- [3] Pradhan A, Baredar O and Kumar A 2015 *Int. j. pure appl. sci. technol.* **5** 51–66
- [4] Bates P R and Dölle K 2017 *IJIRMF* **3** 157-65
- [5] Patuzzi F, Prando D, Vakalis S, Rizzo A M, Chiaramonti D, Tirlir W, Mimmo T, Gasparella A and Barattieri M 2016 *Energy J.* **112** 285–93
- [6] Martinez J D, Mahkamov K, Andrade R V and Lore E E S 2012 *Renew. Energy* **38** 1–9
- [7] Indrawan N, Thapa S, Bhoi P R, Huhnke, Kumar A 2017 *Energy Convers. Manag.* **148** 593–603
- [8] Gobbato P, Massimo M and Benetti M 2015 *Energy Procedia* **82** 149–55
- [9] Shah A, Srinivasan R, To S D F and Columbus E P 2010 *Bioresour. Technol.* **101** 4656–61
- [10] Nadaleti W C and Przybyla G 2018 *Energy J.* **154** 38-51
- [11] Ran Z, Hariharan D, Lawler B and Mamalis S 2019 *Fuel* **235** 530–37
- [12] Hagos F Y, Aziz A R A and Sulaiman S A 2014 *Energy Procedia* **61** 2567–71
- [13] Homdoug N, Tippayawong N and Dussadee N 2015 *Int. J. Appl. Eng. Res.* **9** 2341-8
- [14] Bocci E, Sisinni M, Monetti M, Vecchione L, Di Carlo A and Villarini M 2014 *Energy Procedia* **45** 247-56
- [15] La Villetta M, Costa M, Cirillo D, Massarotti N and Vanoli L 2018 *Energy Convers. Manag.* **175** 33–48
- [16] Pedrazzi S, Santunione G, Minarelli A and Allesina G 2019 *Energy Convers. Manag.* **187** 274–82
- [17] Prestipino M, Salmeri F, Cucinotta F and Galvagno A 2021 *Appl Energy* **295**: 117054
- [18] Golmakani A, Fatemi S and Tamnanloo 2017 *Sep. Purif. Technol* **176** 73–91
- [19] Mivechian Ali and Pakizeh 2013 *Chem. Eng. Technol.* **36** 519–27
- [20] Galvagno A, Prestipino M, Maisano S, Urbani F and Chiodo V 2019 *Energy Conversion and Management* **193**, 74-85
- [21] Fail S, Diaz N, Benedikt F, Kraussler M, Hinteregger J, Bosch K, Hackel M, Rauch R and Hofbauer H 2014 *ACS Sustain. Chem. Eng.* **2** 2690–8
- [22] Famoso F, Prestipino M, Brusca S and Galvagno A. 2020 *Appl Energy* **274**:115315
- [23] Pallozzi V, Di Carlo A, Bocci E, Villarini M, Foscolo P U and Carlini M 2016 *Energy Convers. Manag.* **130**, 34–43
- [24] Prestipino M, Piccolo A, Polito M.F and Galvagno A. 2022 *Energies* **15**:5524
- [25] Carlucci A P, Ficarella A and Laforgia D 2014 *J. Energy Eng.* **140** A4014011 1–8
- [26] Carlucci A P, Colangelo G, Ficarella A, Laforgia D and Strafella L 2015 *J. Energy Eng.* **141**

C4014006 1–8

- [27] Carlucci A P, De Monte V, De Risi A and Strafella L 2017 *J. Energy Eng.* **143** 04017007 1–8
- [28] ISPRA Fattori di emissione per la produzione ed il consumo di energia elettrica in Italia Available online: <http://www.sinanet.isprambiente.it/it/sia-ispra/serie-storiche-emissioni/fattori-di-emissione-per-la-produzione-ed-il-consumo-di-energia-elettrica-in-italia/view>